Journal of the European Ceramic Society 19 (1999) 709–713

PII: S0955-2219(98)00301-X
0955-2219/99/$ - see front matter

Influence of Bi_2O_3/TiO_2, Sb_2O_3 and Cr_2O_3 Doping on Low-voltage Varistor Ceramics

Slavko Bernik,* Petra Zupančič and Drago Kolar

"Jožef Stefan" Institute, Jamova 39, Ljubljana, Slovenia

Abstract

The influence of the amount of Bi_2O_3 and TiO_2 additions at a TiO_2/Bi_2O_3 ratio of 1, as well as Sb_2O_3 and/or Cr_2O_3 doping, on the microstructural development and electrical properties of varistor ceramics in the $ZnO–Bi_2O_3–TiO_2–Co_3O_4–Mn_2O_3$ system was investigated. In samples with a low level of Bi_2O_3 and TiO_2 (0·3 mol%) and therefore small amount of liquid phase, exaggerated growth of the ZnO grains results in high microstructural inhomogeneity. Co-doping with Sb_2O_3 significantly changes the phase composition of TiO_2 doped low-voltage varistor ceramics. The $Bi_3Zn_2Sb_3O_{11}$ type pyrochlore phase forms at the expense of the γ-Bi_2O_3 and $Bi_4Ti_3O_{12}$ phases and decreases the amount of liquid phase in the early stages of sintering. Already small amounts of Sb_2O_3 and/or Cr_2O_3 added to a TiO_2 doped low-voltage varistor ceramics limit ZnO grain growth and increase the threshold voltage V_T of the samples. © *1999 Elsevier Science Limited. All rights reserved*

Keywords: ZnO, varistors, microstructure, grain size, electrical properties.

1 Introduction

Zinc oxide varistors are multicomponent ceramic devices with highly nonlinear current–voltage (*I–V*) characteristics, commonly expressed as $I = KV^{\alpha}$ (K, constant, α, nonlinear coefficient), and high current and energy absorption capabilities. They are widely used as surge absorbers for overvoltage protection and voltage stabilisation in electrical power systems and electronic circuits. The nonlinear characteristic of a ZnO varistor is a grain boundary phenomenon and the break-down voltage of the varistor depends on the number of grain boundaries between the electrodes.[1] For high voltage applications a fine-grained varistor ceramic is required, hence Sb_2O_3 and Cr_2O_3 are commonly added to control the grain growth of ZnO by the presence of a spinel phase at the grain boundaries of ZnO.[2–4] The low voltage ZnO based varistor ceramics are characterized by a coarse-grained microstructure where TiO_2 is commonly used as a grain growth enhancing additive.[5] Peigney *et al.*[6] reported that sintering and grain growth of ZnO depend on the content of Bi_2O_3 as well as the amount of added TiO_2. Our investigations have shown that the TiO_2/Bi_2O_3 ratio significantly influences the microstructural characteristics and the electrical properties of ZnO based varistor ceramics.[7] Depending on the TiO_2/Bi_2O_3 ratio, none, part, or most of the Bi_2O_3 is bounded in the $Bi_4Ti_3O_{12}$ phase and determines the amount of liquid phase below 940°C, therefore coarsening of ZnO grains is able to take place at a relatively low temperature.

In the present work the influence of the amount of Bi_2O_3 and TiO_2 additions at a TiO_2/Bi_2O_3 ratio at 1, as well as Sb_2O_3 and/or Cr_2O_3 doping, on the microstructural development and electrical properties of varistor ceramics in the $ZnO–Bi_2O_3–TiO_2–Co_3O_4–Mn_2O_3$ system was investigated.

2 Experimental

Samples with a nominal composition $(99-2x-y-z)ZnO + xBi_2O_3 + xTiO_2 + 0{\cdot}5Co_3O_4 + 0{\cdot}5Mn_2O_3 + ySb_2O_3 + zCr_2O_3$ were prepared by the classical ceramic procedure to examine the influences of:

a. amount of Bi_2O_3 and TiO_2: compositions for $x = 0{\cdot}9$, 0·7, 0·5 and 0·3 (samples A, B, C, and D, respectively), $y = 0$, $z = 0$;
b. Sb_2O_3 doping: compositions for $x = 0{\cdot}7$, $y = 0{\cdot}04$, 0·12 and 0·20 (samples BS1, BS2 and BS3, respectively), $z = 0$;

*To whom correspondence should be addressed. Fax: +386-61-1263-126; e-mail: slavko.bernik@ijs.si

c. Cr_2O_3 doping: compositions for $x = 0{\cdot}7$, $y = 0$, $z = 0{\cdot}04$, $0{\cdot}12$ and $0{\cdot}20$ (samples BC1, BC2 and BC3, respectively);
d. Sb_2O_3 and Cr_2O_3 doping: compositions for $x = 0{\cdot}7$, $y = 0{\cdot}12$ and $z = 0{\cdot}12$ and $0{\cdot}06$ (samples BSC1 and BSC2, respectively).

All chemicals used were of analytical grade. Discs 8 mm in diameter and 1 mm thick were pressed at 200 MPa and fired at 1260°C for 1 h at heating and cooling rates of 7°C/min in air. Selected samples were also fired at 800°C for 10 h to determine their phase composition at the onset of sintering. Sintering and thermal behaviour of the samples were investigated at a heating rate 10°C/min by dilatometry and differential thermal analysis (DTA), respectively. The phase constitution of the samples was determined by X-ray powder diffraction analysis (XRD). The samples' microstructures were examined by optical and scanning electron microscopy (SEM). Phase compositions of the samples and the composition of the individual phases were analyzed by energy disperse X-ray spectroscopy (EDS). The average ZnO grain size D, its standard deviation σ and the grain size distribution were determined for samples from the measurements on 300–500 grains per sample. The surface of each grain was measured and its size was calculated as a diameter for circular geometry. For DC current–voltage (I–V) characterisation silver electrodes were painted on both surfaces of the disk and fired at 590°C in air. The nominal varistor voltages (V_N) at 1 and 10 mA were measured and the threshold voltage V_T (V/mm) and nonlinear coefficient α were determined.

3 Results and Discussion

The phase composition of characteristic samples after firing at 800 and 1260°C are given in Table 1. In samples A, B, C and D the same phases are present after firing at 800°C, however the amount of γ-Bi_2O_3 and $Bi_4Ti_3O_{12}$ phases decreases from sample A to sample D with decreasing amounts of Bi_2O_3 and TiO_2 in the starting composition. Since the liquid phase in these samples results from the melting of the γ-Bi_2O_3 phase at 820°C and from the reaction between the $Bi_4Ti_3O_{12}$ phase and the Zn–Mn–O phase at 940°C, the amount of liquid phase below 940°C also decreases from sample A to sample D.[7,8] In the sample BC3 Cr is present in the γ-Bi_2O_3 and Zn–Mn–O phases after firing at 800°C. After firing at 1260°C, Cr_2O_3 favours the formation of the $Zn(Ti,Cr)O_{3-\delta}$ type phase instead of Zn_2TiO_4. In the Sb_2O_3 doped samples the $Bi_3Zn_2Sb_3O_{11}$ type pyrochlore phase forms at the expense of the γ-Bi_2O_3 phase and especially the $Bi_4Ti_3O_{12}$ phase. Consequently in sample BS3 with the highest amount of Sb_2O_3, no $Bi_4Ti_3O_{12}$ phase was found after firing at 800°C and TiO_2 is mainly incorporated into the pyrochlore phase. After firing at 1260°C, the ZnO phase, γ-Bi_2O_3 phase, $Bi_3Zn_2Sb_3O_{11}$ type pyrochlore phase and the $Zn_7Sb_2O_{12}$ type spinel phase are present in the sample BS3. In samples BS2 and BS1 with smaller amounts of Sb_2O_3 some $Bi_4Ti_3O_{12}$ phase was also observed. Sb_2O_3 and Cr_2O_3 doped samples BSC1 and BSC2 have similar phase composition as sample BS3 after firing at 800°C. However after firing at 1260°C, Cr_2O_3 stabilises the $Zn_2(Ti,Sb)O_{4-\delta}$ (Cr,Mn,Co) type spinel phase, inhibits the formation of the pyrochlore phase on cooling and enables the $Bi_4Ti_3O_{12}$ phase to precipitate from the Bi_2O_3-rich melt. Microstructures of samples B, BC3 and BS3, fired at 800°C and 1260°C, are shown in Fig. 1.

Dilatometer plots, showing shrinkage of samples with different nominal composition, are compared in Fig. 2. Shrinkage starts at 800°C in samples B, D and BC3 and ends at 950°C in samples B and BC3, and at 1050°C in sample D. In samples BS3 and BSC1 shrinkage starts at 850°C and ends at 1100°C. DT analysis shows an endothermic peak representing melting of the γ-Bi_2O_3 phase at 820°C in samples B and BS3, and at 845°C in samples BC3 and BSC1, indicating that presence of Cr_2O_3 increases the melting temperature of γ-Bi_2O_3. The

Table 1. Phase composition of characteristic samples after firing at 800 and 1260°C

Sample	*800°C*	*1260°C*
B	ZnO, γ-Bi_2O_3 (Zn,Ti) phase, $Bi_4Ti_3O_{12}$, Zn–Mn–O (Ti,Co) phase	ZnO(Co,Mn), γ-Bi_2O_3(Zn, Ti,Co,Mn), Zn_2TiO_4(Mn,Co) phase, $Bi_4Ti_3O_{12}$
BC3	ZnO, γ-Bi_2O_3(Zn,Cr,Ti) phase, $Bi_4Ti_3O_{12}$, Zn–Mn–O (Ti,Co,Cr) phase	ZnO(Co,Mn), γ-Bi_2O_3(Zn,Ti,Co,Mn), $Bi_4Ti_3O_{12}$, $Zn(Ti,Cr)O_{3-\delta}$ (Mn,Co) phase
BS3	ZnO, $Bi_3Zn_2Sb_3O_{11}$ (Ti,Mn,Co) phase, γ-Bi_2O_3 (Zn,Ti) phase	ZnO(Co,Mn), γ-Bi_2O_3(Zn,Ti,Co,Mn), $Zn_7Sb_2O_{12}$(Ti,Co,Mn) phase, $Bi_3Zn_2Sb_3O_{11}$ (Ti,Mn,Co) phase
BSC1	ZnO, $Bi_3Zn_2Sb_3O_{11}$ phase, γ-Bi_2O_3 (Zn,Cr) phase	ZnO(Co,Mn), γ-Bi_2O_3 (Zn,Ti,Co,Mn), $Bi_4Ti_3O_{12}$, $Zn_2(Ti,Sb)O_{4-\delta}$ (Cr,Mn,Co) phase
BSC2	ZnO, $Bi_3Zn_2Sb_3O_{11}$ phase, γ-Bi_2O_3 (Zn,Cr) phase	ZnO(Co,Mn), γ-Bi_2O_3(Zn,Ti,Co,Mn), $Bi_4Ti_3O_{12}$, $Zn_2(Ti,Sb)O_{4-\delta}$ (Cr,Mn,Co) phase

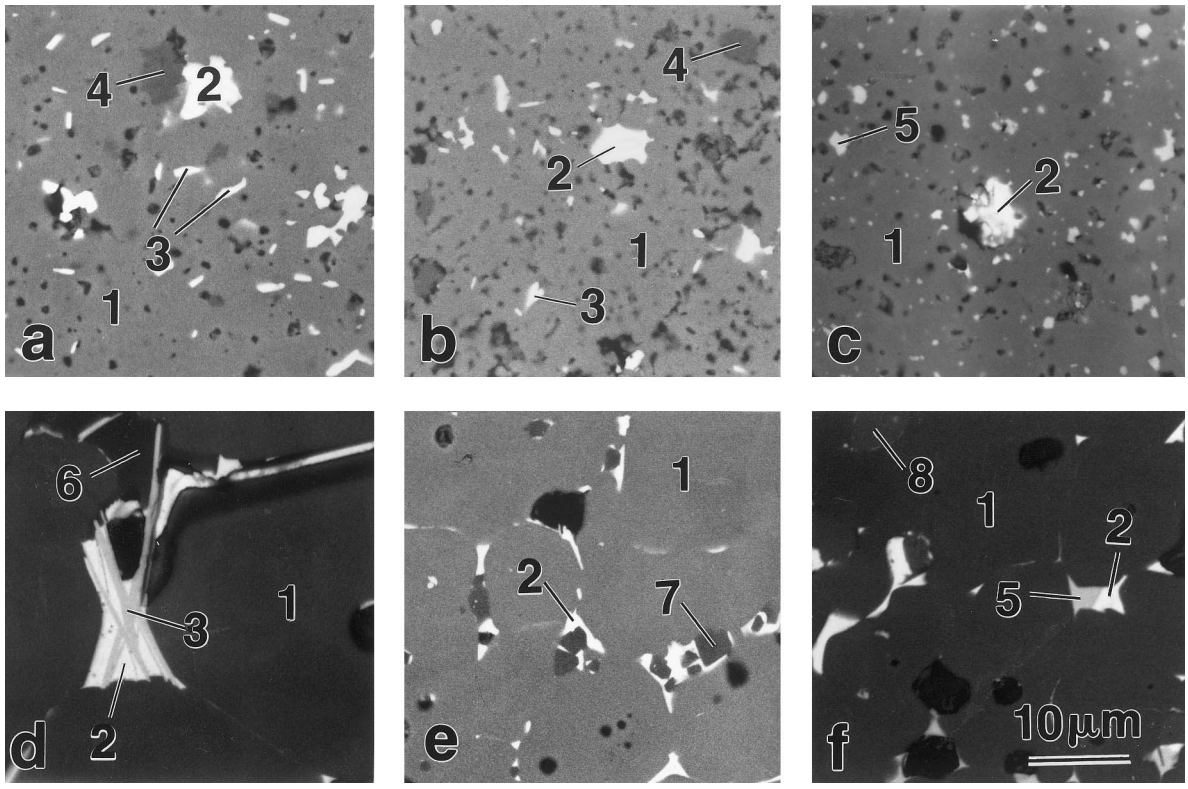

Fig. 1. Backscattered electron (BE) images of samples fired at 800°C: (a) B, (b) BC3, (c) BS3; and 1260°C: (d) B, (e) BC3, (f) BS3; 1: ZnO phase, 2: γ-Bi_2O_3 phase, 3: $Bi_4Ti_3O_{12}$ phase, 4: Zn–Mn–O phase, 5: $Bi_3Zn_2Sb_3O_{11}$ pyrochlore phase, 6: Zn_2TiO_4 phase, 7: $Zn(Ti,Cr)O_{3-\delta}$ phase, 8: $Zn_7Sb_2O_{12}$ spinel phase.

intensities of the endothermic peaks were noticeably smaller for samples BS3 and BSC1 than for samples B and BC3, presumably due to the smaller amount of γ-Bi_2O_3 phase in Sb_2O_3 containing samples.

In pure ZnO, solid phase sintering has already been at 650°C. The presence of additives in the investigated samples shifts the beginning of sintering to a temperature 150°C higher. After formation of a liquid phase the rate of sintering is much faster. This is in agreement with the reports of Peigney *et al.*[6] and others. The results confirm that sintering is influenced by the amount of liquid phase in the sample. Sample B with a higher amount of Bi_2O_3 in the starting composition and

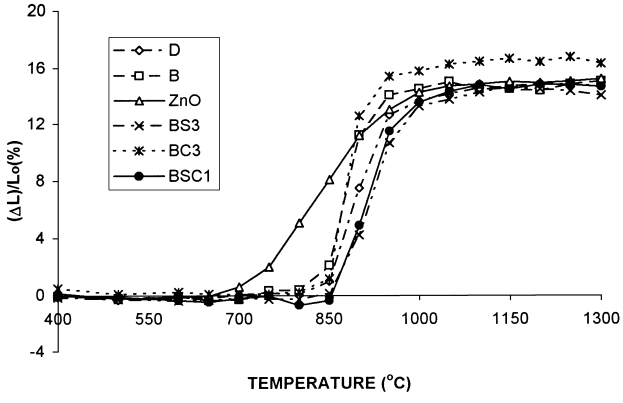

Fig. 2. Densification curves of samples with different starting compositions.

therefore with more liquid phase, has a higher shrinkage rate than sample D. Sample BC3 has similar phase composition to sample B and samples B and BC3 have similar shrinkage curves, which indicates that doping with Cr_2O_3 does not change the amount of liquid phase in the sample BC3 in comparison with sample B. Samples BS3 and BSC1 have the onset of sintering at a higher temperature and they have lower sintering rates. This we ascribe to the formation of the $Bi_3Zn_2Sb_3O_{11}$ type pyrochlore phase in samples BS3 and BSC1. The pyrochlore phase shifts the onset of sintering to higher temperature and bounds a significant amount of Bi_2O_3. The decrease in the amount of free Bi_2O_3 and $Bi_4Ti_3O_{12}$ phase decreases the amount of liquid phase in samples in the early stage of sintering. According to Inada,[2] the pyrochlore phase decomposes above 950°C into the Bi_2O_3-rich liquid phase and $Zn_7Sb_2O_{12}$ phase, while Cho *et al.*[3] reported that some pyrochlore remains and doesn't decompose even at 1100°C, which is higher than the decomposition temperature of $Bi_4Ti_3O_{12}$ phase.

Results of stereological analysis and electrical characterisation of the investigated samples are given in Table 2. Samples A, B, C and D have a similar ZnO grain size, however some extremely large grains with sizes from 100 to over 200 μm are present in sample D with the addition of only 0·3 mol% of Bi_2O_3. Such exaggerated grain growth is well known in systems where a small amount of

Table 2. Results of stereological analysis (average grain size D of ZnO grains and its standard deviation σ) and electrical characterisation (threshold voltage V_T and nonlinear coefficient α) of varistor samples, fired at 1260°C

Sample	*D (μm)*	σ *(μm)*	σ *(%)*	V_T *(V/mm)*	α
A	19	11	58	31	20
B	21	12	57	35	25
C	20	14	70	39	24
D	18	12	67	32	18
BS1	23	15	65	38	34
BS2	19	13	68	44	33
BS3	16	8	50	84	37
BC1	23	12	52	43	20
BC2	21	11	52	51	23
BC3	19	10	53	61	25
BSC1	20	10	50	51	27
BSC2	22	14	63	46	23

liquid phase is present. In the ZnO–Bi_2O_3 system Wong reported exaggerated grain growth of ZnO for additions of Bi_2O_3 in the range 0·05–0·50 mol%.[9] Samples have threshold voltages V_T between 30 V/mm and 40 V/mm and a nonlinear coefficient α from 20 to 25. In Cr_2O_3 doped samples the size of the ZnO grains slightly decreases with increasing amount of Cr_2O_3, while the threshold voltage V_T increases. The $Zn(Ti,Cr)O_{3-\delta}$ type phase is present at the grain boundaries of ZnO in these samples after firing at 1260°C. Since Cr substitutes for a fraction of the Ti in the $Zn(Ti,Cr)O_{3-\delta}$ type phase, it is presumed that the addition of Cr_2O_3 increases the amount of this phase at a certain quantity of TiO_2 in the samples and therefore enhances inhibition of the growth of ZnO grains. The increase in α from 20 to 25 in samples BC indicates only a slight influence of Cr_2O_3 doping on it. In samples doped with Sb_2O_3, growth of ZnO grains is probably inhibited by the presence of the $Bi_3Zn_2Sb_3O_{11}$ type pyrochlore phase and $Zn_7Sb_2O_{12}$ type spinel phase at the grain boundaries of ZnO. Sample BS3 with the highest amount of Sb_2O_3 has the smallest grain size and a much narrower ZnO grain size distribution which results in a significantly higher threshold voltage V_T of this sample in comparison with samples SB1 and SB2. Samples doped with Sb_2O_3 have a nonlinear coefficient α near 35. Microstructures of samples B, D, BS2, BS3, BC2 and BC3, fired at 1260°C, are shown in Fig. 3. Sb_2O_3 and Cr_2O_3 doped samples BSC1 and BSC2 with the Sb_2O_3/Cr_2O_3 ratios of 1 and 2, respectively, have a similar ZnO grain size. However, sample BSC1 has a considerably narrower ZnO grain size distribution than sample BSC2 and therefore higher V_T, probably due to more effective inhibition of ZnO grain growth by a larger amount of $Zn_2(Ti,Sb)O_{4-\delta}$ (Cr,Mn,Co) type phase which results from a larger amount of Sb_2O_3 and Cr_2O_3 in this sample.

4 Summary

Results confirm that sintering and microstructure development are strongly influenced by the amount of liquid phase in the sample. In samples

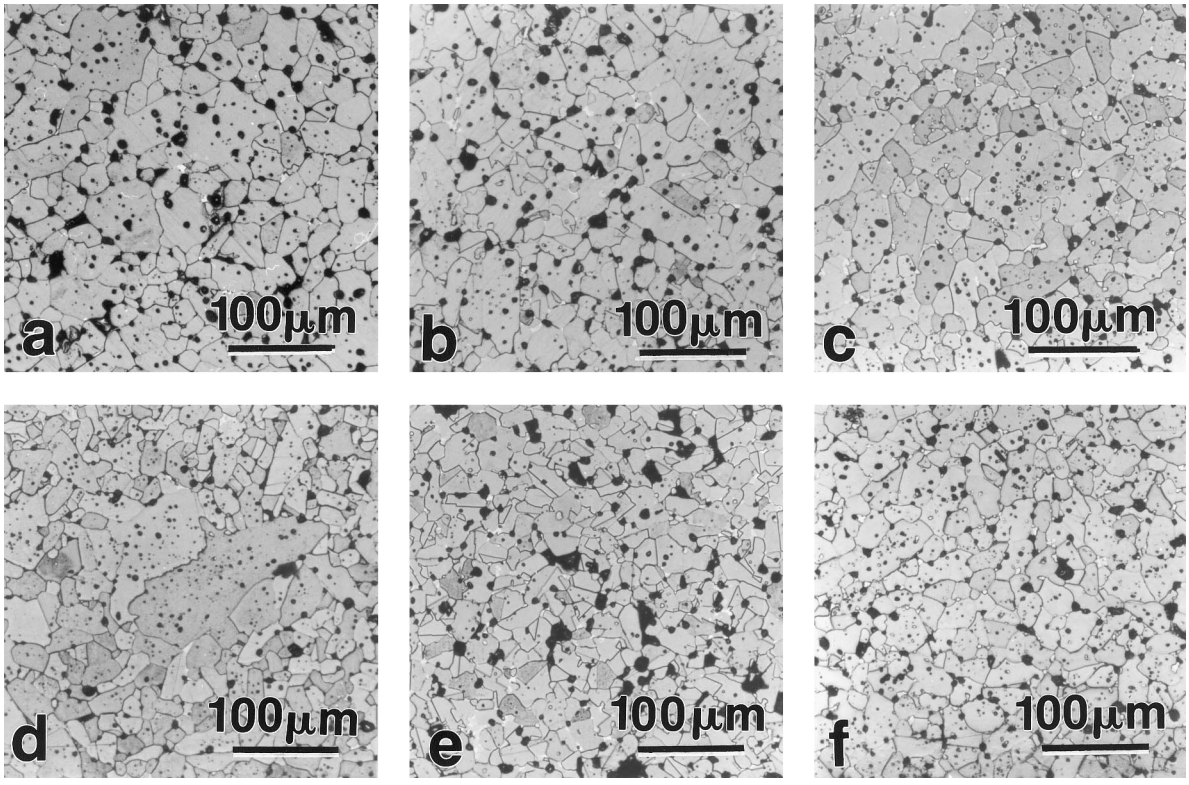

Fig. 3. Optical micrographs of samples fired at 1260°C: (a) B, (b) BS2, (c) BC2, (d) D, (e) BS3 and (f) BC3. Mag. 135×.

with different amounts of Bi_2O_3 and TiO_2 at a TiO_2/Bi_2O_3 ratio of 1, the amount of liquid phase decreases with decreasing amount of Bi_2O_3. The small amounts of liquid phase in the samples with less than 0·5 mol% of Bi_2O_3, result in exaggerated growth of ZnO grains and an inhomogeneous microstructure with some large grains of 100 to over 200 μm in a matrix of smaller grains of ZnO.

Doping with Cr_2O_3 does not significantly influence the phase composition of the samples and therefore the amount of liquid phase in the early stage of sintering in comparison with the samples doped only with Bi_2O_3 and TiO_2 with the same amount of Bi_2O_3 added. The $Zn(Ti,Cr)O_{4-\delta}$ type phase forms in the Cr_2O_3 doped samples at the grain boundaries of ZnO, after firing at 1260°C and its amount increases with increasing amounts of Cr_2O_3. The $Zn(Ti,Cr)O_{4-\delta}$ type phase inhibits the grain growth of ZnO and the threshold voltage V_T of samples increases with increasing amounts of Cr_2O_3.

Already small amounts of Sb_2O_3 significantly change the chemical reactions and the phase composition of TiO_2 doped low-voltage varistor ceramics. In this case microstructure development is characterized by the formation of $Bi_3Zn_2Sb_3O_{11}$ type pyrochlore phase at the expense of the γ-Bi_2O_3 phase and especially the $Bi_4Ti_3O_{12}$ phase. The pyrochlore phase bounds the Bi_2O_3 and TiO_2 and therefore decreases the amount of liquid phase in samples at early stages of sintering which is consequently shifted to a higher temperature. At 0.2 mol% of Sb_2O_3 added, no $Bi_4Ti_3O_{12}$ phase was observed in the sample and the TiO_2 is mainly incorporated in the pyrochlore phase. In Sb_2O_3 doped samples the growth of ZnO grains is inhibited by the presence of $Bi_3Zn_2Sb_3O_{11}$ type pyrochlore phase and the $Zn_7Sb_2O_{12}$ type spinel phase at the grain boundaries of ZnO and the threshold voltage V_T significantly increases for an increase in the amount of Sb_2O_3 from 0·12 mol% to 0·20 mol%. Sb_2O_3 doping results in a higher nonlinear coefficient α. In these samples the pyrochlore phase is also stable after firing at 1260°C. However, in Sb_2O_3 and Cr_2O_3 doped samples, Cr_2O_3 stabilises the $Zn_2(Ti,Sb)O_{4-\delta}$ (Cr,Mn,Co) type spinel phase, inhibits the formation of the pyrochlore phase on cooling and the $Bi_4Ti_3O_{12}$ phase precipitates from the Bi_2O_3-rich melt.

Acknowledgements

The work was supported by INCO-COPERNICUS Program of the European Commission within the project HIPOVAR; IC15-CT96-0749. The financial support of the Ministry of Science and Technology of Slovenia is also gratefully acknowledged.

References

1. Gupta, T. K., Application of zinc oxide varistors. *J. Am. Ceram. Soc.*, 1990, **73**, 1817–1840.
2. Inada, M., Formation mechanism of nonohmic zinc oxide ceramics. *Jpn. J. Appl. Phys.*, 1980, **19**, 409–419.
3. Cho, S. G., Lee, H. and Kim, S. K., Effect of chromium on the phase evolution and microstructure of ZnO doped with bismuth and antimony. *J. Mater. Sci.*, 1997, **32**, 4283–4284.
4. Kraševec, V., Trontelj, M. and Goliè, L., Transmission electron microscope study of antimony doped zinc oxide ceramics. *J. Am. Ceram. Soc.*, 1991, **74**, 760–766.
5. Trontelj, M., Kolar, D. and Krašovec. V., Influence of additives on varistor microstructures, In *Advances in Ceramics, Vol. 7, Additives and Interfaces in Electronic Ceramics*, ed. M. F. Yan and A. H. Heuer. The American Ceramic Society, Columbus, OK, 1983, pp. 107–116.
6. Peigney, A., Andrianjatovo, H., Legros, R. and Rousset, A., Influence of chemical composition on sintering of bismuth-titanium-doped zinc oxide. *J. Mater. Sci.*, 1992, **27**, 2397–2405.
7. Bernik, S., Microstructural and electrical characteristics of ZnO based varistor ceramics with varying TiO_2/Bi_2O_3 ratio. *The Proceedings of CIMTEC'98 World Ceramic Congress & Forum on New Materials*, Florence, Italy, 1998, submitted for publication.
8. Makovec, D., Trontelj, M., Formation reactions of low-voltage varistor ceramics. In *Materials Science Monographs, 66C, Ceramics Today—Tomorrow's Ceramics*, ed. P. Vincenzini. Elsevier Science, Amsterdam 1991, pp. 2137–2145.
9. Wong, J., Sintering and varistor characteristics of ZnO–Bi_2O_3 ceramics. *J. Appl. Phys.*, 1980, **51**, 4453–4459.